Available online at www.sciencedirect.com
ScienceDirect
Polymer 48 (2007) 4385–4392
polymer
www.elsevier.com/locate/polymer

Silica/poly(*N*,*N*′-methylenebisacrylamide) composite materials by encapsulation based on a hydrogen-bonding interaction

Guangyu Liu [a,b], Xinlin Yang [a,*], Yongmei Wang [b]

[a] *Key Laboratory of Functional Polymer Materials, The Ministry of Education, Institute of Polymer Chemistry, Nankai University, Tianjin 300071, China*

[b] *Department of Chemistry, Nankai University, Tianjin 300071, China*

Received 10 March 2007; received in revised form 1 May 2007; accepted 24 May 2007
Available online 29 May 2007

Abstract

Monodisperse silica/poly(*N*,*N*′-methylenebisacrylamide) core–shell composite materials with silica as core and poly(*N*,*N*′-methylenebisacrylamide) (PMBAAm) as shell were prepared by a two-stage reaction, in which the silica core with diameter of 500 nm was synthesized in the first stage according to Stöber method. The PMBAAm shell was then encapsulated over the silica core by distillation–precipitation polymerization of *N*,*N*′-methylenebisacrylamide (MBAAm) in neat acetonitrile with 2,2′-azobisisobutyronitrile (AIBN) as initiator. The encapsulation of PMBAAm on silica particles was driven by the hydrogen-bonding interaction between the hydroxyl group on the surface of silica core and the amide unit of PMBAAm during the polymerization without modification of the silica surface in the absence of any stabilizer or surfactant. The shell thickness of the core–shell composite particle was controlled via altering the mass ratio of MBAAm monomer to silica core during the polymerization. Hollow PMBAAm microsphere was further developed after removal of silica core with hydrofluoric acid. The resultant core–shell composite and hollow microspheres were characterized by scanning electron microscopy (SEM), transmission electron microscopy (TEM), Fourier-transform infrared spectra (FT-IR) and elemental analysis (EA).

Keywords: Inorganic–organic composite particle; Distillation–precipitation polymerization; Core–shell composite

1. Introduction

In recent years, the combination of the properties of inorganic and organic building blocks within a single material has attracted rapidly expanding interest for material scientists because of the possibility to combine the various functional groups of organic components with the advantages of a thermally stable and robust inorganic substrate [1,2]. These composite materials can exhibit novel and excellent properties, such as mechanical, chemical, electrical, rheological, magnetic, optical and catalytic, by varying the compositions, dimensions, and structures of the core and shell, which have promised diverse applications as drug delivery system, diagnostics, coatings, and catalysis [3–9].

The silica/polymer hybrid particles with various interesting morphologies, such as silica core/organic shell [10], organic core/silica shell [11], raspberry-like [12], snowman-like [13], daisy-shaped and multipod-like [14], and raisinbun-like [15], have been prepared by different methods. The synthesis of the silica/polymer hybrid particles can be generally classified as two categories: the self-assembly of the resultant silica and polymer particles via physical or physicochemical interaction, and the direct polymerization of monomer on the surface of silica particles. Kulbaba et al. [16,17] assembled positively charged polyferrocenylsilane microspheres with negatively charged silica particles through the electrostatic forces. Layer-by-layer [18–22] deposition technique by sub-sequential adsorption of polyelectrolytes (PEs) with opposite charges onto silica particles via the electrostatic interaction has been reported for the preparation of a range of polymer-core/inorganic-shell particles. Fleming et al. [8] fabricated raspberry-like composites

* Corresponding author. Tel.: +86 22 23502023; fax: +86 22 23503510.
E-mail address: xlyang88@nankai.edu.cn (X. Yang).

0032-3861/$ - see front matter © 2007 Elsevier Ltd. All rights reserved.
doi:10.1016/j.polymer.2007.05.060

from silica microspheres and polystyrene nanospheres by either the reaction of amine and aldehyde groups or the biochemical interaction between avidin and biotin. Bourgeat-Lami et al. [23–25] synthesized silica/organic hybrid particles with silica as seeds by dispersion polymerization, in which the vinyl group was introduced by 3-(trimethoxysilyl)propyl methacrylate. The hedgehog-like or raspberry-like hybrid particles were prepared by miniemulsion polymerization [26], in which the silica nanoparticles acted as surfactants and fillers. Bourgeat-Lami et al. [27] synthesized silica/poly(methyl methacrylate) nanocomposite particles by emulsion polymerization with a cationic initiator 2,2′-azobis(isobutyraidine) dihydrochloride (AIBA·2HCl) in the presence of a nonionic polyoxyethelenic surfactant (NP30). However, it was difficult to control the morphology of the resultant silica/polymer hybrid particles and the encapsulation efficiencies of the polymer on the silica core were much low for both dispersion polymerization and emulsion polymerization. Surface-initiated atom transfer radical polymerization (ATRP) has been widely utilized to prepare well-defined silica/polymer hybrids with the initiator-modified silica particles as macroinitiators [28–31], in which the synthesis was tedious with long reaction time and low conversion of monomer to polymer.

We have previously reported distillation–precipitation polymerization as a novel and powerful technique to prepare monodisperse poly(divinylbenzene) (polyDVB) [32], poly (ethyleneglycol dimethacrylate) (polyEGDMA) [33], poly (*N*,*N*′-methylenebisacrylamide) (polyMBAAm) [34] and other polymer microspheres with various functional groups [35–37]. In the present work, monodisperse silica/polyMBAAm core–shell composite materials were prepared by distillation–precipitation polymerization with silica particles as seeds in the presence of 2,2′-azobisisobutyronitrile (AIBN) as initiator in neat acetonitrile, in which polyMBAAm was encapsulated onto silica particles with the aid of the hydrogen-bonding interaction between the hydroxyl group on the surface of silica and the amide unit of polyMBAAm. Furthermore, hollow polyMBAAm microspheres were developed after removal of the silica cores by hydrofluoric acid.

2. Experimental

2.1. Chemicals

Tetraethyl orthosilicate ($Si(OC_2H_5)_4$, TEOS) was purchased from Aldrich and used without any further purification. *N*,*N*′-Methylenebisacrylamide (MBAAm, chemical grade, Tianjin Bodi Chemical Engineering Co.) was recrystallized from acetone. 2,2′-Azobisisobutyronitrile (AIBN) was available from Chemical Factory of Nankai University and recrystallized from methanol. Hydrofluoric acid (HF, containing 40 wt% of HF) was available from Tianjin Chemical Reagent Institute. Acetonitrile (analytical grade, Tianjin Chemical Reagents II Co.) was dried over calcium hydride and purified by distillation before use. All the other reagents were of analytical grade and used without any further purification.

2.2. Synthesis of silica core

Silica particles were prepared according to the classical Stöber method [38]. TEOS of 7 mL was added to the mixture of 200 mL ethanol and 55 mL of 25% ammonium aqueous solution with vigorous stirring at room temperature and the reaction was continued further for 24 h with stirring. The resultant silica particles were then purified by three cycles of centrifugation, decantation, and resuspension in ethanol with ultrasonic bath. The silica particles were dried in a vacuum oven at 50 °C till constant weight.

2.3. Preparation of silica/polyMBAAm composite materials by distillation–precipitation polymerization

A typical procedure for the distillation–precipitation polymerization: in a dried 100-mL two-necked flask, 0.2 g silica particles were suspended in 80 mL of acetonitrile as a white suspension. Then MBAAm (0.2 g, total as 0.25 wt% of the reaction system) and AIBN (0.004 g, 2 wt% relative to the monomer) were dissolved in the suspension. The two-necked flask fitted with a fractionating column, Liebig condenser and receiver was placed in a heating mantle. The reaction mixture was heated from ambient temperature till the boiling state within 20 min and the reaction system was kept under reflux for further 10 min. The white color was deepened during heating and the solvent was then distilled off the reaction system within 1.5 h. After the polymerization, the resulting silica/polyMBAAm composite material was purified by repeating centrifugation, decantation, and resuspension in acetone with ultrasonic bath for three times. The particles were then dried in a vacuum oven at 50 °C till constant weight.

The other distillation–precipitation polymerizations were much similar to that of the typical procedure by varying the weight ratio of MBAAm to silica particles while the amount of AIBN initiator was maintained at 2 wt% relative to the monomer. The treatment of these composite particles was the same as that for the typical process. The reproducibility of the polymerizations was confirmed through several duplicate and triplicate experiments.

2.4. Synthesis of hollow polyMBAAm microspheres

The resultant silica/polyMBAAm core–shell composite particles were immersed in 40% hydrofluoric acid solution for 2 h. Then the excess HF and the formed SiF_4 were expelled out of the reaction system. The hollow polyMBAAm microspheres were purified by several centrifugation/washing cycles in water till pH 7. The resultant polyMBAAm hollow microspheres were dried in a vacuum oven at 50 °C till constant weight.

2.5. Characterization

The size and size distribution of silica/polyMBAAm core–shell composite materials were determined by scanning electron microscopy (SEM, Philips XL-30) and the morphologies

of the silica core, the resultant hollow polyMBAAm microspheres were characterized by transmission electron microscopy (TEM, Tecnai G2 20 S-TWIN). All the size and size distribution reflect the averages about 100 particles each, which are calculated according to the following formula:

$$U = D_w/D_n \quad D_n = \sum_{i=1}^{k} n_i D_i / \sum_{i=1}^{k} n_i \quad D_w = \sum_{i=1}^{k} n_i D_i^4 / \sum_{i=1}^{k} n_i D_i^3$$

where U is the polydispersity index, D_n is the number-average diameter, D_w is the weight-average diameter, and D_i is the particle diameter of the determined microparticles.

Fourier-transform infrared spectra (FT-IR) were scanned over the range of 400–4000 cm^{-1} with potassium bromide plate on a Bio-Rad FTS135 FT-IR spectrometer.

Elemental analysis (EA) was performed on a Perkin–Elmer-2400 to determine the nitrogen, carbon and hydrogen contents of the resultant samples.

3. Results and discussion

The TEM micrograph of silica from a sol–gel process as shown in Fig. 1A indicated that the silica particles had

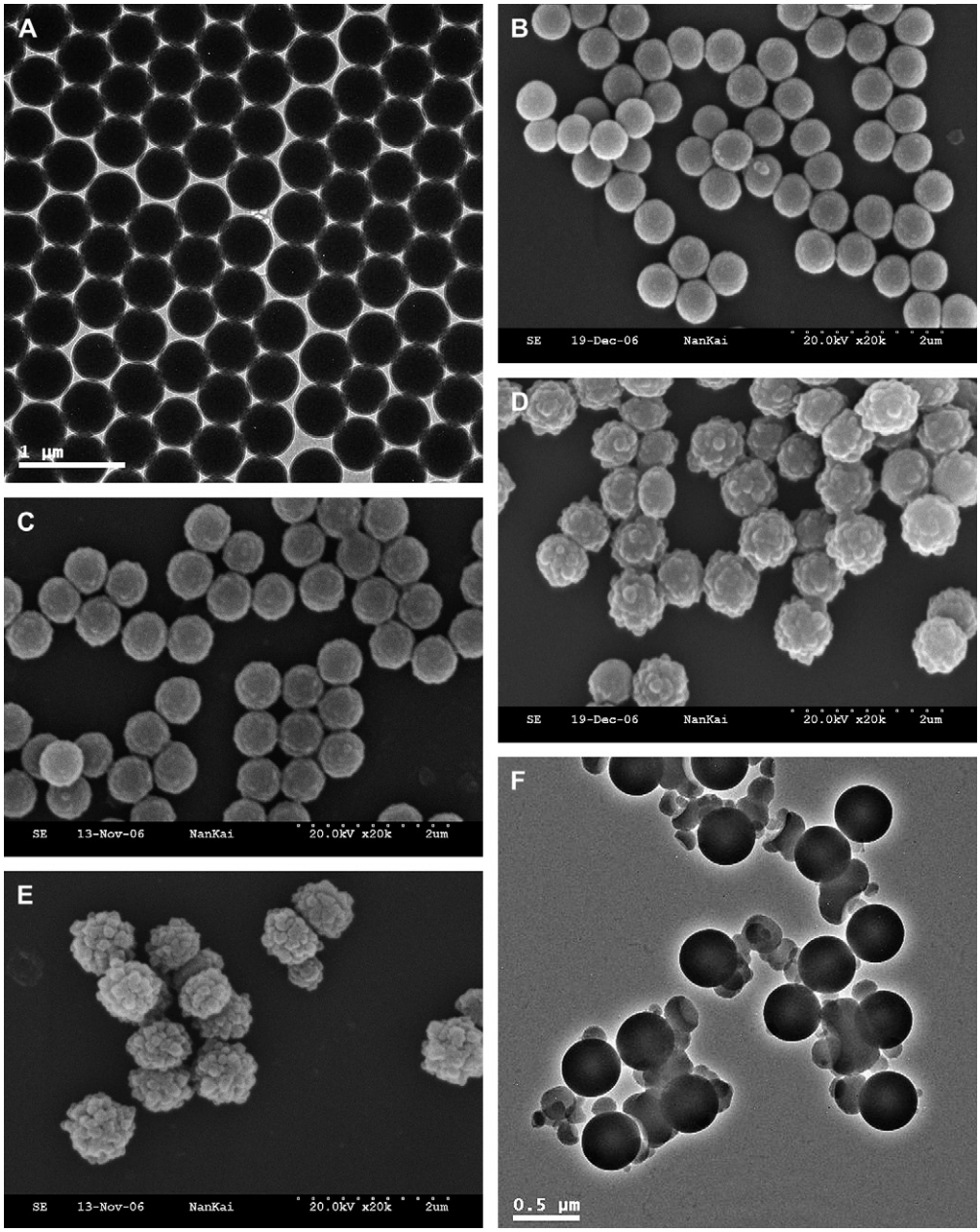

Fig. 1. Micrograph of microspheres: (A) TEM micrograph of silica particles; (B–E) SEM micrographs of silica/polyMBAAm microspheres with different MBAAm feed during polymerization as mass ratio to silica core: (B) 1/2; (C) 1/1; (D) 3/2; (E) 2/1; (F) TEM micrograph of irregular PDVB particles in the presence of silica particles as seeds. Reaction conditions: 80 mL of acetonitrile and AIBN as initiator of 2 wt% relative to the monomer.

a spherical shape with an average size of 500 nm and monodispersity index (U) of 1.008.

The residual double bonds on the polyDVB core were essential to afford monodisperse core–shell functional microspheres by two-stage distillation–precipitation polymerization [37], in which the newly formed oligomers were captured by the active carbon–carbon double bonds without the second-initiated particles during the second-stage polymerization. In the present work, the surface of silica seeds has only active hydroxyl groups in the absence of carbon–carbon double bonds without any modification. The hydrogen-bonding has much effect on the crystallization behavior of poly(3-hydroxybutyrate-*co*-2-hydroxyhexanoate)/silica hybrid composites [39]. In our previous paper, the hydrogen-bonding interaction has played an active role during the distillation–precipitation polymerization in neat acetonitrile while involving the hydrophilic comonomers, such as acrylic acid [40], MBAAm and *N*-isopropylacrylamide (NIPAm) [34]. Here, we utilized this technique to afford monodisperse silica/polyMBAAm composite particles with regular shape, in which the hydrogen-bonding interaction between the hydroxyl group on the surface of silica and the amide group of polyMBAAm would promote the encapsulation of polyMBAAm on silica particles.

3.1. Preparation of silica/polyMBAAm core–shell composite

Monodisperse silica/polyMBAAm core–shell composite was prepared by the second-stage distillation–precipitation polymerization of MBAAm in neat acetonitrile with AIBN as initiator as illustrated in Scheme 1, in which the silica particles with active hydroxyl groups were used as seeds for the growth of the shell layer. The previous results indicated that acetonitrile met the solvency conditions required for the formation of monodisperse polyMBAAm microspheres with regular shape by distillation–precipitation polymerization, that is, it dissolved the MBAAm monomer, but precipitated the forming polyMBAAm [34]. The essential role of the hydrogen-bonding for the formation of monodisperse polymer microspheres was confirmed by our previous work in the case of polymerization of the hydrophilic monomers involving the hydrogen-bonding, such as MBAAm and NIPAm [34], acrylic acid [35,40]. The SEM micrographs of the resultant silica/polyMBAAm core–shell composite materials with different thickness of shell layer are shown in Fig. 1, which were afforded by controlling the amount of MBAAm feed during the second-stage polymerization with acetonitrile as the solvent. In the present work, the shell thickness was calculated as the half of the difference between the diameter of the final core–shell microspheres and that of silica core.

The SEM micrographs indicated that the core–shell composites had spherical shape with smooth surface in the case of low MBAAm feed (Fig. 1B and C), and rough surfaces in the presence of high MBAAm loading (Fig. 1D and E). The formation of cauliflower-like silica/polyMBAAm core–shell particles with rough surfaces in the case of high MBAAm monomer during the second-stage polymerization may originate from the structure and the high reactivity of the MBAAm monomer. The reactive divinyl groups in MBAAm were connected by the flexible methylene and diamide groups, which led to the residual double bonds on the surfaces of silica/polyMBAAm particles being scarce during the polymerization. It was reported that the residual vinyl groups on the surface of polymer microspheres were essential to result in the monodisperse polymer microspheres through the capture of the newly formed oligomers for the growth of the microspheres for precipitation polymerization [41] and distillation–precipitation polymerization [32]. The absence of the active vinyl groups on the surface of silica/polyMBAAm particles was proven further by FT-IR spectra as shown in Fig. 2c without a typical peak at 1630 cm^{-1} corresponding to the stretching vibration of the double bonds. This implied that the capability of the residual double bonds on the silica/polyMBAAm composite surface was not enough to capture efficiently all the newly formed oligomers from the solution during the polymerization. On the other hand, the strong hydrogen-bonding interaction between the polyMBAAm species in the presence of amide groups in acetonitrile promoted them by attracting each other and aggregating together quickly during the polymerization, as the acetonitrile was a non-protonic polar solvent not interfering in the hydrogen-bonding interaction. As a result, the cauliflower-like silica/polyMBAAm particles with rough surfaces were

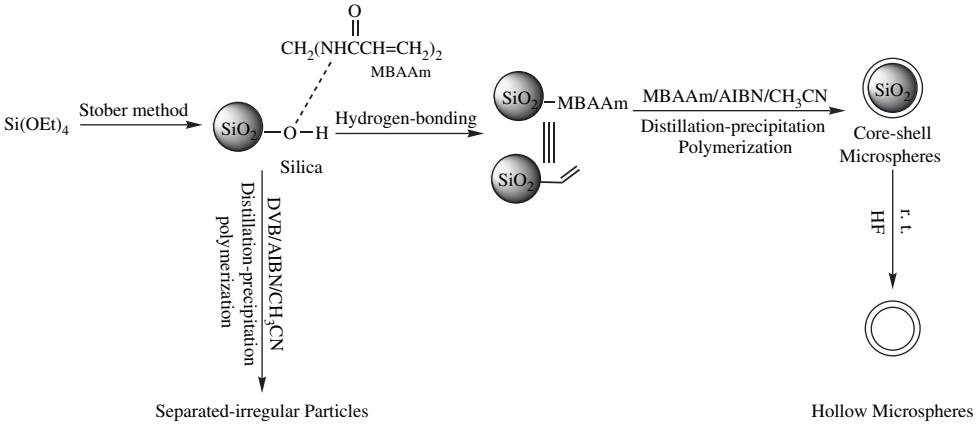

Scheme 1. Preparation and mechanism for the formation of silica/PMBAAm composite materials.

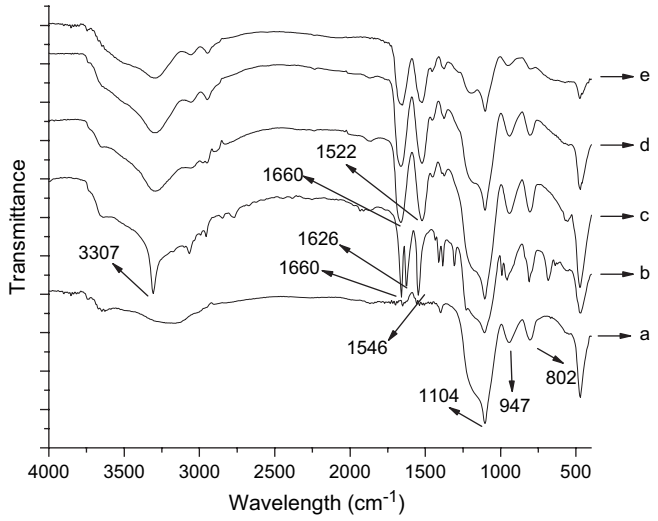

Fig. 2. FT-IR spectra of silica and silica/polyMBAAm composite materials with different MBAAm feed during the polymerization as mass ratio to silica core: (a) silica particles; (b) mixture of silica and MBAAm monomer before polymerization after washing with acetonitrile for three times; (c) silica/polyMBAAm (1/2); (d) silica/polyMBAAm (1/1); (e) silica/polyMBAAm (2/1). Reaction conditions: 80 mL of acetonitrile and AIBN as initiator of 2 wt% relative to the monomer.

formed, especially in the case of high loading of MBAAm monomer.

The experimental conditions for the distillation–precipitation polymerization of MBAAm with silica particles as seeds, the size, size distribution and the yield of the resultant silica/polyMBAAm composite materials are summarized in Table 1. The size of the core–shell composite materials increased significantly with increasing MBAAm loading in the polymerization system. The maximum diameter of 864 nm was obtained when the ratio of MBAAm to silica (in mass) was 2/1. This meant that the thickness of the shell layer were in the range of 19–182 nm with the MBAAm feed ranging from 1/2 to 2/1 (in mass ratio to silica particles). The monodisperse core–shell composites were obtained with the polydispersity index (U) in the range of 1.006–1.017, which depended on the ratio of MBAAm monomer to silica cores during the polymerization. The formation of cauliflower-like composite particles resulted in the broader size distribution with high MBAAm loading as discussed above. The narrowest silica/polyMBAAm particles with polydispersity index (U) of 1.006 and diameter of 538 nm were prepared at a MBAAm feed of 1/2 (in mass ratio to silica cores). The yield of the final silica/polyMBAAm core–shell microspheres indicated in Table 1 remained higher than 94% irrespective to the MBAAm feed changing from 1/2 to 2/1 (in mass ratio of silica core), which was consistent with the increasing thickness from SEM characterization and the linear increasing N content in the final core–shell microspheres as shown in Fig. 3. In other words, polyMBAAm was quantitatively encapsulated on the surface of silica core with the aid of hydrogen-bonding interaction between the hydroxyl group on the surface of silica core and the amide group of polyMBAAm component, which was much higher than the encapsulation efficiencies of dispersion polymerization [23–25] and emulsion polymerization [27] in the literature.

3.2. The mechanism of formation for silica/polyMBAAm core–shell composite

The monodisperse silica/polyMBAAm core–shell composite was formed without any second-initiated particles after the second-stage polymerization, in which the thickness of the polyMBAAm shell was controlled through the feed of the MBAAm monomer. These results indicated that all the polyMBAAm species were exclusively encapsulated over the silica cores. In the present work, the encapsulation of polyMBAAm onto the silica cores was driven by the hydrogen-bonding interaction between the active hydroxyl group and the amide unit of polyMBAAm species during the polymerization as shown in Scheme 1. Hydrogen-bonding interaction has been widely used as a driving force to afford multilayer films of weak polyelectrolytes (PEs) [42–44] and raspberry-like core-corona polymer composite [45], which are very sensitive to pH changes due to the presence of electrostatic repulsion between the components for the formation of films and composites.

To understand the hydrogen-bonding interaction mode for the present distillation–precipitation polymerization, FT-IR spectra were measured for silica core, the silica adsorbed with MBAAm before polymerization, and the silica/polyMBAAm core–shell composites with different shell thickness as shown in Fig. 2.

Table 1
The size, size distribution, yield, shell thickness and nitrogen content of silica/polyMBAAm particles, the fraction of polymer component in composites with different recipe in the feed[a]

Entry	SiO_2 (g)	MBAAm (g)	D_n (nm)	D_w (nm)	U	Shell thickness (nm)	Nitrogen content (wt%)	Fraction[c] (%)	Yield[d] (%)
A[b]	0.2	0	500	504	1.008	0	0	0	0
B	0.2	0.1	538	541	1.006	19	5.91	32	96
C	0.2	0.2	602	608	1.010	51	8.29	45	94
D	0.2	0.3	742	751	1.012	121	10.39	58	97
E	0.2	0.4	864	879	1.017	182	12.71	66	98

[a] Reaction conditions: 80 mL of acetonitrile and AIBN as initiator of 2 wt% relative to the total monomers.
[b] Silica core.
[c] Fraction = $(M_{core-shell} - M_{hollw})/M_{core-shell} \times 100\%$.
[d] Yield = $(M_{core-shell} - M_{silica})/M_{monomer} \times 100\%$.

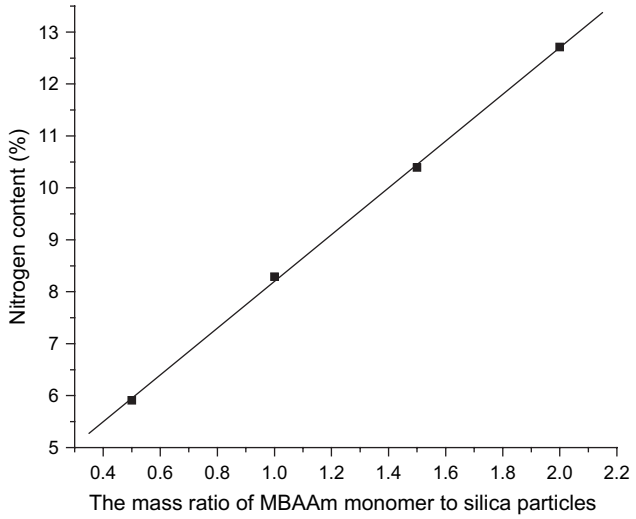

Fig. 3. Relationship between nitrogen weight content of the silica/PMBAAm composite materials and the mass ratio of MBAAm monomer to silica particles in the feed.

For silica core particles, the FT-IR spectrum (Fig. 2a) had a strong peak at 1104 cm^{-1} and a middle peak at 802 cm^{-1} corresponding to the symmetrical and asymmetrical stretching vibration of Si–O–Si with a middle peak at 947 cm^{-1} attributing to the stretching vibration of hydroxyl group. The FT-IR spectrum (Fig. 2b) for the mixture of silica and MBAAm after repeated centrifugation, decantation and resuspension in acetonitrile was determined to investigate the strong adsorption of MBAAm monomer on the surface of silica cores with the aid of the hydrogen-bonding interaction between the hydroxyl groups on the surface of silica cores and the amide groups in MBAAm monomer. There were new peaks in Fig. 2b at 3307, 1660, 1626 and 1546 cm^{-1} corresponding to the stretching vibration of N–H bond, carbonyl and vinyl groups, and the bending vibration of N–H bond, with a simultaneous decrease in peak at 947 cm^{-1} assigning to the stretching vibration of the hydroxyl group. In other words, hydrogen-bonding interaction played a key role as the driving force during the encapsulation of polyMBAAm on silica cores with initial incorporation of the reactive vinyl groups. Then the adsorbed vinyl groups on the surface of silica microspheres captured the newly formed oligomers for the encapsulation of polyMBAAm for the growth of silica/polyMBAAm composite particles, which was similar to the role for the vinyl groups during the precipitation polymerization [41] and distillation–precipitation polymerization [32,37].

The essential role of the hydrogen-bonding interaction for the polymerization was confirmed further by the formation of separated-irregular particles (Fig. 1F) in the presence of silica particles as seeds for the polymerization of divinylbenzene (DVB), in which the DVB monomer cannot be encapsulated onto the silica cores due to its hydrophobic nature lacking the hydrogen-bonding interaction with the silica particles.

The surface modification of polyMBAAm resulting in silica/polyMBAAm core–shell composites was studied further by FT-IR spectra as shown in Fig. 2. The FT-IR spectra (curves c–e in Fig. 2) of silica/polyMBAAm particles showed the expected strong peaks at 3300, 1660, 1522 cm^{-1} corresponding to the stretching vibration of N–H bond, carbonyl groups, and the bending vibration of N–H bond due to the encapsulation of polyMBAAm. The peak at 1626 cm^{-1} disappeared completely in these core–shell composites proving the high reactivity of the vinyl groups of polyMBAAm species as discussed above. The FT-IR spectra of silica/polyMBAAm composites showed a significant increase in the intensity of both carbonyl stretching at 1660 cm^{-1} and the bending vibration of N–H bond at 1522 cm^{-1} compared to that of the stretching vibration of Si–O–Si at 1104 cm^{-1}, while the MBAAm feed was increased from 1/2 to 2/1 (in mass ratio to silica core) during the polymerization. These results indicated that the amount of polyMBAAm encapsulated over the silica cores increased significantly with increasing loading of MBAAm monomer, which was consistent with the results from SEM observation in Fig. 1B–E.

Furthermore, the nitrogen content of the resultant silica/polyMBAAm composites from elemental analysis (EA) increased significantly from 5.91 to 12.71% (Table 1), when the mass ratio of MBAAm monomer to silica particles in the feed was increased from 1/2 to 2/1. The nitrogen content in silica/polyMBAAm composites increased linearly with the amount of MBAAm monomer feed during the polymerization as shown in Fig. 3, which confirmed further the efficient encapsulation of polyMBAAm over silica cores due to the high reactivity of MBAAm monomer.

3.3. Synthesis of polyMBAAm hollow microspheres

In our previous work, the crosslinked PDVB core in the core–shell structure polymer microspheres [37] cannot be selectively removed for the preparation of the corresponding hollow polymer microspheres. Silica cores of the resultant silica/polyMBAAm core–shell composites were selectively removed by etching of silica core in hydrofluoric acid to afford polyMBAAm microspheres. The driving force for such removal was due to the formation of SiF_4 gas, which was given off from the microspheres during the etching to afford polyMBAAm hollow microspheres. The TEM micrographs of polyMBAAm hollow microspheres with different thickness are illustrated in Fig. 4.

When the MBAAm monomer feed during the polymerization was as low as 1/2 (mass ratio to silica core), the results in Fig. 4A with several collapsed particles indicated that the shell layer was not thick (around 19 nm) enough to support the cavities formed during the selective dissolution of silica cores. The monodisperse hollow polyMBAm microspheres shown in Fig. 4B and C were obtained with MBAAm feed in the range of 1/1 to 3/2 (mass ratio to silica core), in which the convincing hollow-sphere structures were observed with the presence of circular rings of non-aggregated spheres and a cavity in the interior. The size of the shell layer for the resultant polyMBAAm hollow microspheres was estimated from TEM characterization increasing from 51 to 121 nm as summarized in Table 1, when MBAAm loading was increased from 1/1

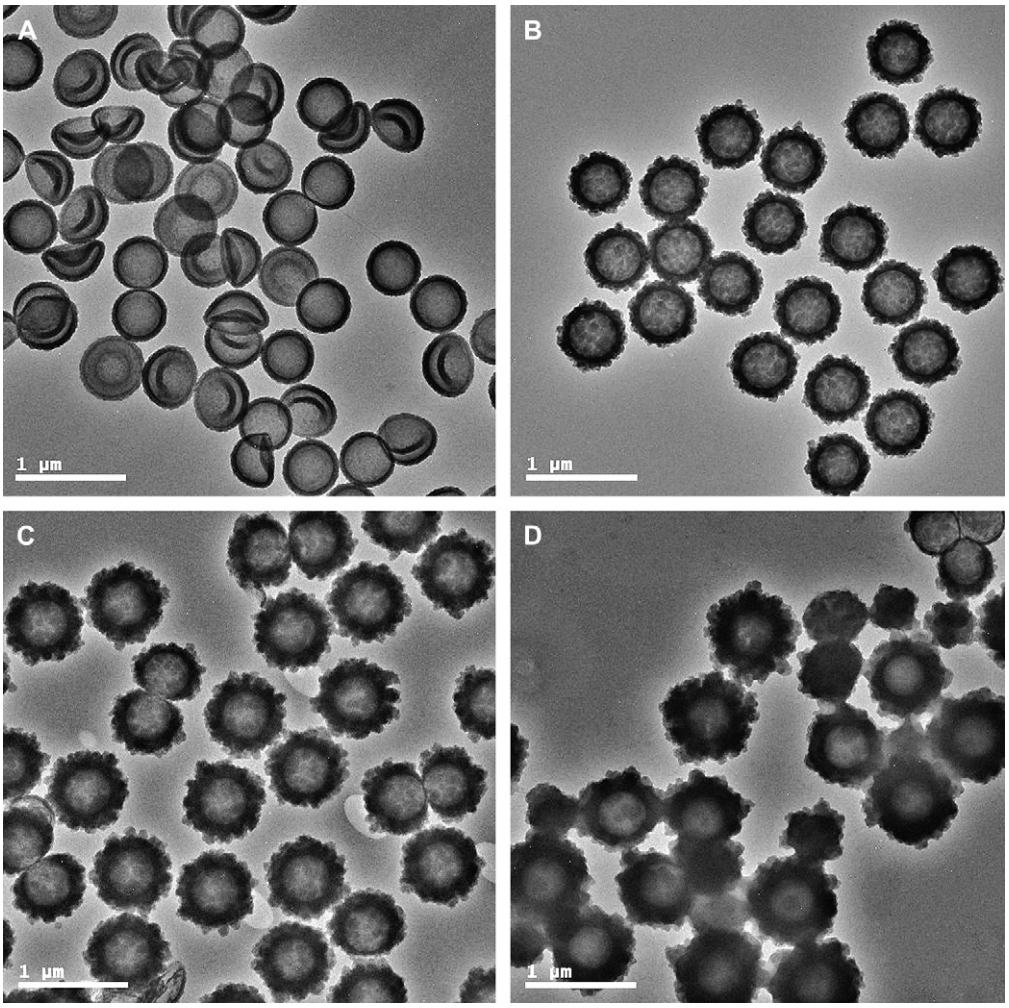

Fig. 4. TEM micrographs of polyMBAAm hollow microspheres with different shell thickness by altering the MBAAm feed during the distillation–precipitation polymerization: (A) 1/2; (B) 1/1; (C) 3/2; (D) 2/1 (in mass ratio to silica core).

to 3/2 (mass ratio to silica core) during the distillation–precipitation polymerization. In short, the shell thickness of the resultant polyMBAAm hollow microspheres can be conveniently controlled by altering the amount of MBAAm monomer feed during the formation of the shell layer by distillation–precipitation polymerization. However, when the MBAAm loading for the polymerization was increased further to 2/1 (mass ratio to silica core), hollow polyMBAAm microspheres with the shell thickness around 182 nm were afforded as shown in Fig. 4D, in which a few second-initiated small polyMBAAm particles were observed. This was due to the formation of cauliflower-like silica/polyMBAAm core–shell structure with rough surfaces as discussed above, in which the capture ability of the composite particles was not enough during the polymerization in the case of high MBAAm loading as 2/1 (in mass ratio to silica core).

The fraction of the polymer component was obtained from the mass difference of silica/polyMBAAm and the corresponding polyMBAAm hollow microspheres after selective removal of silica core as listed in Table 1. The fraction of polymer component decreased significantly from 66 to 32% when the MBAAm feed during the polymerization was decreased from 2/1 to 1/2 (mass ratio to silica core). These results confirmed further the successful removal of silica core by hydrofluoric acid during the etching process. The synthesis of the other core–shell structure silica/polymer microspheres and the corresponding hollow polymer microspheres is in progress, which would prove the present synthesis route as a general method for other polymer systems.

4. Conclusion

Monodisperse silica/polyMBAAm core–shell composites with regular shape were prepared by distillation–precipitation polymerization of MBAAm in neat acetonitrile with silica particles as seeds and AIBN as initiator in the absence of any additive. The hydrogen-bonding interaction between the active hydroxyl groups on the surface of silica particles and the amide groups of MBAAm played a key role for the efficient encapsulation of polyMBAAm over the silica cores. The thickness of polyMBAAm shell layer and the morphology of the resultant silica/polyMBAAm composites were controlled by the MBAAm monomer feed during the polymerization. The polyMBAAm hollow microspheres with shell thickness

in the range of 51–121 nm were further developed by the selective etching of the silica cores in hydrofluoric solution from silica/polyMBAAm core–shell composites. The study on the scope of this technique, including the extension to the other inorganic–organic composites through the encapsulation of the other inorganic particles, such as magnetite, zirconia, tin(IV) oxide, titania oxide, is in progress.

Acknowledgements

This work was supported in part by the National Science Foundation of China (Project No.: 20504015) and the Opening Research Fund from the State Key Laboratory of Polymer Chemistry and Physics, Chinese Academy of Sciences (Project No.: 200613).

References

[1] Zhang YD, Lee SH, Yoonessi M, Liang KW, Pittman CU. Polymer 2006;47:2984.
[2] Strachotova B, Strachota A, Uchman M, Slouf M, Brus J, Plestil J, et al. Polymer 2007;48:1471.
[3] Zhu J, Morgan AB, Lamelas FJ, Wilkie CA. Chem Mater 2001;13:3774.
[4] Caruso F, Spasova M, Susha A, Giersig M, Caruso RA. Chem Mater 2001;13:109.
[5] Cho JD, Ju HF, Hong JH. J Polym Sci Part A Polym Chem 2005;43:658.
[6] Zhou J, Zhang SW, Qiao XG, Li XQ, Wu LM. J Polym Sci Part A Polym Chem 2006;44:3202.
[7] Luzinov I, Xi K, Pagnoulle C, Huynh-Ba G, Jerome R. Polymer 1999;40:2511.
[8] Fleming MS, Mandal TK, Walt DR. Chem Mater 2001;13:2210.
[9] Hu YQ, Wu HP, Gonsadves KE, Merhari L. Microelectron Eng 2001;56:289.
[10] Zhang K, Chen HT, Chen X, Chen ZM, Cui ZC, Yang B. Macromol Mater Eng 2003;288:380.
[11] Tissot I, Novat C, Lefebvre F, Bourgeat-Lami E. Macromolecules 2002;34:5737.
[12] Reculusa S, Poncet-Legrand C, Ravaine S, Minogotaud S, Duguet E, Bourgeat-Lami E. Chem Mater 2002;14:2354.
[13] Derro A, Reculusa S, Bourgeat-Lami E, Duguet E, Ravaine S. Colloid Surf A 2006;284–285:78.
[14] Reculusa S, Mingotaud C, Bourgeat-Lami E, Duguet E, Ravaine R. Nano Lett 2004;4:1677.
[15] Barthlet C, Hickey AJ, Carins DB, Armes SP. Adv Mater 1999;11:408.
[16] Kulbaba K, Resendes R, Cheng A, Bartole A, Safa-Senat A, Coombs N, et al. Adv Mater 2001;13:732.
[17] Kulbaba K, Cheng A, Bartole A, Greenberg S, Resendes R, Coombs N, et al. J Am Chem Soc 2002;124:12522.
[18] Caruso F, Caruso AA, Möhwald H. Science 1998;282:400.
[19] Caruso F. Adv Mater 2001;13:11.
[20] Caruso RA, Susha A, Caruso F. Chem Mater 2001;13:400.
[21] Caruso F, Caruso RA, Möhwald H. Chem Mater 1999;11:3309.
[22] Caruso F, Lidenfeld H, Giersig M, Möhwald H. J Am Chem Soc 1998;120:8523.
[23] Bourgeat-Lami E, Lang J. J Colloid Interface Sci 1998;197:293.
[24] Bourgeat-Lami E, Lang J. J Colloid Interface Sci 1999;210:281.
[25] Corcos F, Bourgeat-Lami E, Novat C, Lang J. Colloid Polym Sci 1999;277:1142.
[26] Tiarks F, Landfester K, Antonietti M. Langmuir 2001;17:5775.
[27] Lula-Xavier JL, Guyot A, Bourgeat-Lami E. J Colloid Interface Sci 2001;250:82.
[28] von Werne T, Patten TE. J Am Chem Soc 1999;121:7409.
[29] von Werene T, Patten TE. J Am Chem Soc 2001;123:7497.
[30] Perruchot C, Khan MA, Kamitsi A, Armes SP. Langmuir 2001;17:4479.
[31] Harrak AE, Carrot G, Oberdisse J, Jestin J, Boue F. Polymer 2005;46:1095.
[32] Bai F, Yang XL, Huang WQ. Macromolecules 2004;37:9746.
[33] Bai F, Yang XL, Huang WQ. Eur Polym J 2006;42:2088.
[34] Liu GY, Yang XL, Wang YM. Polym Int 2007;56:905.
[35] Bai F, Yang XL, Li R, Huang B, Huang WQ. Polymer 2006;47:5775.
[36] Lu XY, Huang D, Yang XL, Huang WQ. Polym Bull 2006;56:171.
[37] Qi DL, Bai F, Yang XL, Huang WQ. Eur Polym J 2005;41:2320.
[38] Stöber W, Fink A. J Colloid Interface Sci 1968;26:62.
[39] Lim JS, Noda I, Im SS. Polymer 2007;48:2745.
[40] Bai F, Yang XL, Huang WQ. Chin J Polym Sci 2006;24:163.
[41] Li WH, Stöver HDH. Macromolecules 2000;33:4354.
[42] Kato T, Frechet JMJ. Macromolecules 1989;22:3818.
[43] Stockron WB, Rubner MF. Macromolecules 1997;30:2717.
[44] Zhang HY, Wang ZQ, Zhang YQ, Zhang X. Langmuir 2004;20:9366.
[45] Li R, Yang XL, Li GL, Li SN, Huang WQ. Langmuir 2006;22:8127.